AFCRL-68-0357

NUMERICAL METHODS OF COMPUTING THREE-DIMENSIONAL TRAJECTORIES FOR ADIABATIC AND DIABATIC FLOWS

J. D. Mahlman
Dept. of Meteorology and Oceanography
Naval Postgraduate School
Monterey, California 93940

NPS-51MZ8061A; SR-3

Research Project MIPR ES-7-967
Project No.   6698
Task No.   669802
Work Unit No. 66980201

Scientific Report No. 3
August 1968

Contract Monitor: Thomas Keegan, Meteorology Laboratory

Prepared for

AIR FORCE CAMBRIDGE RESEARCH LABORATORIES
OFFICE OF AEROSPACE RESEARCH
UNITED STATES AIR FORCE
BEDFORD, MASSACHUSETTS 01730

NUMERICAL METHODS OF COMPUTING THREE-DIMENSIONAL TRAJECTORIES FOR ADIABATIC AND DIABATIC FLOWS

J. D. Mahlman
Dept. of Meteorology and Oceanography
Naval Postgraduate School
Monterey, California 93940

NAVAL POSTGRADUATE SCHOOL
Monterey, California

Rear Admiral R. W. McNitt, USN
Superintendent

R. F. Rinehart
Academic Dean

July 1968

Abstract

A computer method for objective computation of adiabatic three-dimensional trajectories in the free atmosphere is presented. This technique utilizes a digital adaptation of the graphical iterative method introduced by Danielsen (1961).

The program is applied to a test case and is found to give generally satisfactory results. Some difficulties are encountered in cases of very low wind speeds and also in regions of strong anticyclonic wind shears.

A method for inclusion of diabatic effects is outlined in detail. This approach may allow investigation of more complicated flow problems than have been previously possible.

1. Introduction

The determination of three dimensional trajectories by air parcels in the free atmosphere has been of interest to meteorologists for many years. Knowledge of parcel trajectories is valuable in analysis of trace substance transports, in the diagnosis of large scale systems, and also can be of importance in weather forecasting.

Although the large scale motion of the atmosphere is overwhelmingly horizontal, it has long been recognized that neglection of the vertical velocity component can produce appreciable trajectory errors in as little as 12 hours (e.g., see Petterssen, 1956). However, since the large scale vertical motion must be inferred rather than measured directly, progress has been very slow in developing satisfactory trajectory techniques.

Because diabatic effects in non-precipitating regions are generally accepted to be quite small in the free atmosphere, the concept of evaluating trajectories on isentropic surfaces has long been an appealing one (Panofsky, 1947; Saucier, 1955; Petterssen, 1956). Many different techniques have been used previously -- the most straightforward being a direct graphical calculation from isotach and streamline analyses (Palmén and Newton, 1951; Danielsen, 1959; Reiter and Danielsen, 1960; Staley, 1960, 1962; Reiter, 1963).

In any trajectory scheme the accuracy of the computed displacement tends to degenerate rather seriously with time. This is due to the

1

uncertainty inherent in basic data which is only available in discrete form in both space and time. Calculations of trajectories by the above method directly from streamline and isotach analyses are particularly difficult due to the extreme sensitivity of the calculation to errors in the streamline analyses. For example, a wind direction error of just 10° can produce a normal displacement from the true trajectory of about 2° latitude in just 12 hours under average wind conditions. The effects of errors of this type and of radiosonde spacing errors were pointed out by Djuric (1961).

In an attempt to minimize the uncertainty due to streamline errors, Danielsen (1961) developed a more objective technique based upon a path integration of the total energy equation expressed in isentropic coordinates. This basic graphical technique has subsequently been used with good results by Danielsen (1964), Danielsen, Bergman, and Paulson (1962), Houghton (1962), Mahlman (1965), and by Reiter and Mahlman (1965a, b, c). This approach has been used in tracing movement of radioactive debris, with computed results in agreement with observed transports.

2. Methods of computing three-dimensional trajectories

As noted in the previous section the energy method developed by Danielsen (1961) has proven to be an effective technique for obtaining three dimensional trajectories in the free atmosphere. A basic difficulty in employing this system is the time of computation involved. Initially, isentropic surfaces must be generated containing analyzed

2

wind and Montgomery stream function ($c_p T + gZ$) information. An excellent treatment of the problems involved in obtaining Montgomery stream functions on isentropic surfaces is given by Danielsen (1959). Next, in the evaluation of the trajectories, a graphical iterative scheme is employed. This becomes very time consuming and cumbersome when a large number of trajectories must be determined.

One way to avoid this difficulty without loss of computational accuracy is to perform the calculations with a digital computer rather than by graphical methods. This, of course, is advantageous in that any such technique is completely objective, once it is successfully programmed. Several previous investigators have developed computer techniques for evaluating three dimensional trajectories.

Nagle and Clark (1966) employed a kinematic scheme on isentropic surfaces using the sum of the geostrophic wind and a divergent wind inferred from the continuity equation expressed in isentropic coordinates. This procedure may not yield the most satisfactory results because the divergent part of the wind field inferred by this method may be far from reliable. Also, Krishnamurti (1966a) showed that appreciable ageostrophic wind components are mostly non-divergent. This difficulty could possibly be reduced by using the balance equation to deduce the non-divergent stream function.

Paegle (1966) computes three-dimensional trajectories kinematically in a pressure coordinate system using a vertical motion (ω) in the

3

vertical and the sum of a non-divergent and divergent wind in the hori-

zontal. The non-divergent stream function (ψ) is obtained from the non-

linear form of the balance equation. The velocity potential (χ) is ob-

tained from the vertical motion field. This vertical motion field is derived

by a succession of iterations of the complete non-linear omega equation

(Krishnamurti, 1966b). This technique contains the possibility of giving

excellent results provided that the derived three dimensional winds are

not overly sensitive to errors in the initial height field and further, are

not excessively smoothed during the complex numerical procedures. In

fact, part of the objective of this study is to develop an alternative

trajectory method to this one in order to provide more rigorous tests

for each approach. This is particularly important, since both schemes

are very complex numerically, and require considerable preparation of

input data.

In the usual kinematic trajectory scheme one integrates the equations

$$d \phi = \frac{v}{a} \, dt \tag{1}$$

$$d \lambda = \frac{u}{a \cos \phi} \, dt$$

where ϕ is the latitude, λ the longitude, u and v the horizontal

scaler velocity components, and a is the radius of the earth. Because the

u and v velocity components are either explicitly or implicitly derived

from the analyses of streamlines and isotachs, errors in streamlines

can produce appreciable errors in the final trajectory positions. In the

free atmosphere the wind shears normal to the flow are generally much

larger than those along the flow. As a result of this, streamline errors producing computed trajectory positions normal to the true position are especially serious.

A way to reduce the problems associated with this difficulty would be to devise an objective method which "constrains" the parcel from deviating so far laterally from its true position. The graphical method proposed by Danielsen (1961) is specifically designed to provide this constraint by using the additional information given by the distribution of thermodynamic variables.

Because this graphical method has produced highly reliable results, a proper computer simulation of this technique should also prove to be reliable. The rest of this section will discuss the concept behind this method and demonstrate how it is done on a computer rather than graphically.

Since this method is so fundamental to the subsequent development of the machine method, the basic concepts of this system will be presented here.

The horizontal equation of motion in isentropic coordinates is

$$\frac{d\vec{V}_2}{dt} = - f \vec{k} \times \vec{V}_2 - \nabla_\theta M + \vec{F} \tag{2}$$

where V_2 is the horizontal wind vector, f the Coriolis parameter, $\vec{k}$ a unit vector in the vertical, ∇_θ the two dimensional gradient operator on a surface of constant potential temperature θ, M the Montgomery

stream function, and $\vec{F}$ is the friction force.

Taking the dot product of the horizontal wind vector into Eq. (2) gives

$$\frac{d}{dt}\left(\frac{\vec{V}_2 \cdot \vec{V}_2}{2}\right) = -\vec{V}_2 \cdot \nabla_\theta M + \vec{V}_2 \cdot \vec{F}, \tag{3}$$

the mechanical energy equation expressed in θ coordinates. Performing an Eulerian expansion on the first term and noting that $-\vec{V}_2 \cdot \nabla_\theta M = -\frac{dM}{dt}_\theta + \frac{\partial M}{\partial t}_\theta$,

$$\frac{d}{dt}\left(\frac{\vec{V}_2 \cdot \vec{V}_2}{2}\right)_\theta + \frac{d\theta}{dt}\frac{\partial}{\partial\theta}\left(\frac{\vec{V}_2 \cdot \vec{V}_2}{2}\right) = -\frac{dM}{dt}_\theta + \frac{\partial M}{\partial t}_\theta + \vec{V}_2 \cdot \vec{F}. \tag{4}$$

The substantial derivatives with θ subscripts now represent the substantial derivative computed without the vertical advection term.

If Eq. (4) is now integrated over the time interval Δt, one obtains

$$
\overset{(1)}{(M_F - M_i)_\theta} = \overset{(2)}{-\left(\frac{v_f^2 - v_i^2}{2}\right)_\theta} + \overset{(3)}{\int_{t_i}^{t_f}\frac{\partial M}{\partial t}_\theta \, dt} \tag{5}
$$

$$
\underset{(4)}{-\int_{\theta_i}^{\theta_f}\frac{\partial}{\partial\theta}\left(\frac{v^2}{2}\right)d\theta} + \underset{(5)}{\int_{t_i}^{t_f}\vec{V}\cdot\vec{F}\,dt},
$$

where the i and f subscripts represent the initial and final values, respectively, and $v^2 = \vec{V}_2 \cdot \vec{V}_2 = u^2 + v^2$. The left hand side of Eq. (5) represents the change of the Montgomery stream function over the time interval of the projection of the true trajectory onto the θ surface. The first term on the right hand side of Eq. (5) (term 2) is the change

6

of kinetic energy of the projected trajectory. Term (3) represents the

integrated local M tendency along the trajectory path. Term (4) is the

change of kinetic energy on the original θ surface due to non-adiabatic

motions. Finally, term (5) is the work done on the mass of air by friction.

Eq. (5) is now in a form such that it can be used to produce a better

approximation to the final trajectory point. In general, this equation

must be solved iteratively since the final value of M determined from

it is a function of the true trajectory path. Eq. (5) thus serves to provide

a constraint on the deviations of a computed trajectory normal to its true

position resulting from streamline errors. Since the Montgomery stream

function on a θ surface is exactly analogous to the geopotential height

on a pressure surface, a restraint on the permissible values of M_f

provides a satisfactory method for reducing the error of a computed tra-

jectory.

In graphically computed isentropic trajectories the usual procedure

is to determine the first approximation to the true trajectory by evalua-

ting Eq. (1) in the integrated form

$$S = \overline{V} \Delta t, \tag{6}$$

where S is the displacement and $\overline{V}$ is the average wind speed along

the trajectory over the interval Δt . The information from this initial

approximation is then used to compute a value of M_f from Eq. (5)

with terms 4 and 5 omitted. If the computed value of M_f from Eq. (5)

differs from the value of M_f measured from the initial trajectory, the

initial trajectory is then displaced laterally until the final point on the chart satisfies the computed value of M_f. At this point Eq. (6) is re-evaluated along the new path to correct for possible changes in wind speeds along this new path. This new trajectory is then used to re-compute the terms in Eq. (5). If the computed and actual values agree within predetermined limits (usually $\sim .1 \times 10^7$ erg/g), the trajectory is completed. If not, the process is repeated until the desired accuracy is reached.

Even though, in general, air movement in the free atmosphere is neither frictionless or adiabatic, it is commonly accepted that these assumptions are approximately valid over short periods of time. According to Kung (1967) a reasonable value of energy dissipation in the free atmosphere is 2.3 erg g^{-1} sec^{-1} or .01 x 10^7 erg g^{-1} 12 hr^{-1}. If this value is compared with the typical values of .5 x 10^7 erg g^{-1} $12hr^{-1}$ for terms 1, 2, and 3 in Eq. (5), its neglection is clearly justified. However, in the surface layer its effect becomes more important. The effect of neglecting diabatic motions is at times more serious. Inclusion of these effects will be discussed in detail in section 4.

3. Machine adaptation of the energy integral method

The previous section has shown how the energy equation expressed in θ coordinates can be used to obtain more accurate three-dimensional trajectories in the atmosphere. Because of its utility this system has been adapted for solution on the computer by digital rather than graphical

8

methods. Due to the requirement of an iterative solution to this problem, there exists an almost unlimited number of approaches which could prove successful. The method employed here will be described in some detail to illustrate one solution to the problem.

Although the longer range goal is to apply the technique to the generalized problem including diabatic flows (see section 4) the initial programming is restricted to the case of isentropic flow. This produces an appreciable simplification in the original programming logic.

All calculations are performed on a Cartesian grid of arbitrary size and spacing. The spacing between grid points is fixed in degrees latitude and longitude. Because of this, the actual spacing in the east-west direction is a function of latitude. Basic constants read in are the latitude-longitude spacing between grid points, the southern latitude and western longitude boundaries, number of grid points in the x and y directions, number of levels in the vertical, and number of time steps to be calculated. The initial variables read in are wind direction, wind speed, pressure, and Montgomery stream function at each point in the 4-dimensional (x, y, θ, t) grid.

The first computational step is to convert the velocity field to u and v components. Also, the variation of the grid point spacing along the x-axis and of the Coriolis parameter with increasing latitude is determined. Next, the u and v fields are linearly interpolated to give values at times between the 12 hour observation times used for the input data. A simple difference is taken to obtain the local 12 hour

9

Montgomery stream function tendency. At present this 12 hour difference is assumed to be representative of the tendency over the entire 12 hours. In future programs higher order interpolation schemes will be employed. This will be at considerable difficulty due to the additional data tabulations necessary and increased machine storage requirements.

The first approximation to the final trajectory is obtained by a rather straightforward kinematic approach. Beginning at a grid point the parcel is displaced for one hour using the initial values of u and v to determine the length and direction of the displacement. At this point the time interpolated u and v values are spatially interpolated from the nearest four grid points to the parcel to obtain u and v wind components for the parcel at its new position. These new u and v values are then used to extrapolate the parcel for another hour, at which time new u and v components are again found. This process is repeated until the 12 hour time is reached.

At each point along the trajectory a test is made to determine whether the parcel has left the original grid. If the parcel is found to be outside this data field, the trajectory is terminated and a new trajectory is begun at the next starting grid point. If the parcel remains within the grid, preparations are begun for the iterative phase of the computation using the adiabatic, frictionless form of Eq. (5). Values of

kinetic energy and Montgomery stream function are calculated at the initial and final points of the 12 hour trajectory. Also, the finite difference form of the local Montgomery stream function tendency is interpolated at each point and then summed to get a mean tendency along the 12 hour trajectory.

It might be noted that this initial approximation to the trajectory can provide a valid result as long as the original wind fields have been adequately specified and the time interpolations are satisfactory. As a separate problem it is of interest to note the differences between these original, kinematically determined trajectories and the final ones which also satisfy the energy equation.

To begin the iteration the difference is obtained between the value of M_f computed from Eq. (5) with terms (4) and (5) omitted and M_f obtained from the actual trajectory (δM). If the absolute value of this difference is less than $.05 \times 10^7$ erg g^{-1}, the initial trajectory is assumed to be correct and the calculation proceeds to a new trajectory. If this is not the case, the trajectory is then corrected in the direction of reducing this difference. This is accomplished by noting that in θ coordinates,

$$V_g = -\frac{1}{f} \frac{\partial M}{\partial n}_\theta \qquad (7)$$

where V_g is the total geostrophic wind and n is the coordinate directed normal to the M lines. A "correction distance" can be determined from (7) in the finite difference form

11

$$\delta n = \frac{-\delta M}{f V_s} \tag{8}$$

Note that V_s, the actual wind, is used rather than the geostrophic wind here. This value of δn obtained from Eq. (8) must then be translated into λ and ϕ displacements so that the exact direction of the iteration can be determined. Since the correction must be made <u>normal</u> to the trajectory path, this is accomplished by the expressions

$$\delta \lambda = \frac{\delta n}{a \cos \phi} \frac{v}{V_s} \qquad \delta \phi = \frac{\delta n}{a} \frac{u}{V_s} , \tag{9}$$

where u, v, and V_s are evaluated at the final point of the first approximation to the trajectory.

One may note that this technique does not completely eliminate the difference between the two values of M_f unless the flow is geostrophic. However, the flow may deviate far from the geostrophic and the method will still move the trajectory in the proper direction for convergence. If the angle between streamlines and Montgomery stream function contours is greater than 90°, the method would fail. Since this condition is extremely rare in the free atmosphere, the method proves to be generally effective.

Once $\delta \lambda$ and $\delta \phi$ have been determined for the final point, each point along the trajectory is displaced a distance proportional to $\delta \lambda$ and $\delta \phi$ depending upon its time of occurrence along the 12 hour trajectory (eg., $\delta \lambda_{1 \text{ hr.}} = \frac{1}{12} \delta \lambda, \delta \lambda_{9 \text{ hr.}} = \frac{9}{12} \delta \lambda$).

At this point a new approximation to the trajectory has been completed.

12

However, this new approximation to the trajectory may be in a somewhat different wind speed regime, thus necessitating an additional correction. This is accomplished by writing

$$\delta s = S_{wind} - S_{geom},$$ (10)

where δs is the distance correction (to be made parallel to the trajectory). S_{wind} is the total displacement along the new trajectory obtained by summing 1 hour displacements using the total wind at each point. S_{geom} is the distance obtained by summing the actual geometric distances between the 1 hour trajectory points. Thus δs provides a correction for the actual wind speed in the vicinity of the new trajectory. Note that this is only a correction for the speed and does <u>not</u> correct for direction. This value of δs is then converted to λ and ϕ displacements according to

$$\delta \lambda = -\frac{\delta s}{a \cos \phi} \frac{u}{V_s} \qquad \qquad \delta \phi = \frac{\delta s}{a} \frac{v}{V_s}$$ (11)

At this point the trajectory has been corrected for the Montgomery stream function change plus an additional correction for distance. The difference between M_f computed from the adiabatic, frictionless form of Eq. (5) along the new trajectory and the value of M_f actually measured from the trajectory end point is then recomputed. If the absolute value of this difference is now less than $.05 \times 10^7$ erg g^{-1}, the trajectory is complete. If not, the iterative cycle is repeated until convergence is reached.
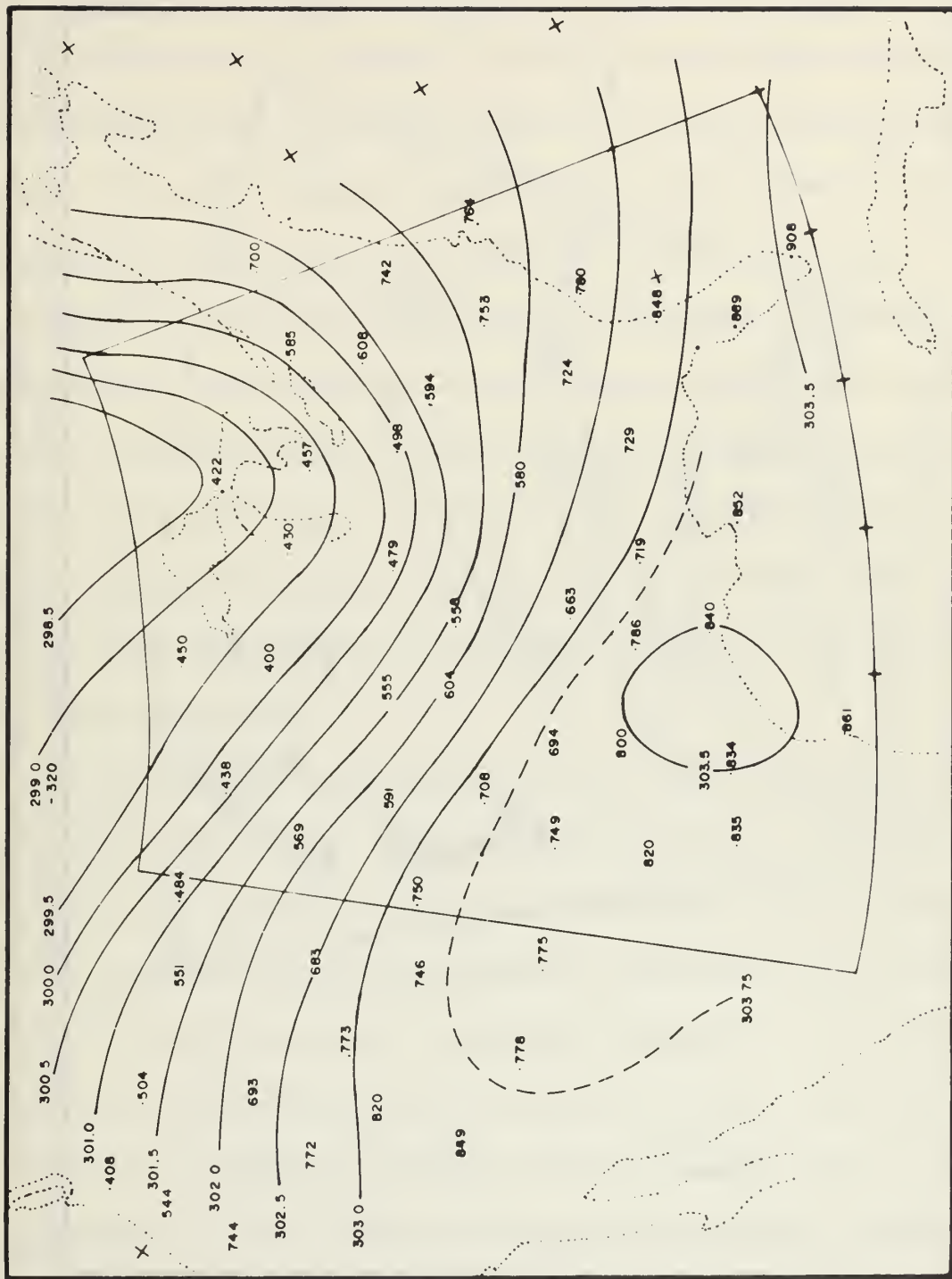
Normally, the iterative correction for a 12 hour trajectory is not particularly large (usually less than 2° latitude). However, in certain

situations when appreciable accelerations are present, or the large

scale systems are moving rapidly, the corrections can be substantial.

Fig. 1 is an analysis of Montgomery stream function (10^7 erg g^{-1})

for a trajectory test case at θ = 300K, beginning 22 November 1962,

1200 GMT. Pressures at θ = 300K are given in mb.

A sample of some of the adiabatic trajectories obtained from the

machine method outlined above are given in Fig. 2 for the 12 hour period

beginning on 22 November 1962, 1200 GMT. The dashed lines are the

kinematic trajectories used as a first approximation to the final tra-

jectories. The solid lines represent the 12 hour trajectories obtained by

the energy integral method. A single solid line emanating from a point

means that the kinematic trajectory also satisfied the energy integral

condition. The two types of trajectories tend to be similar -- the

iterated trajectory normally characterized by a small lateral correction

to the kinematic one.

A marked exception to this general characteristic may be seen in the

lower left trajectory in Fig. 2. In this case the iterated trajectory is

displaced almost perpendicularly from the kinematic trajectory. The

cause of this difficulty may be seen in Fig. 1, which shows that this is

an area of very weak M gradients. Because the lateral distance cor-

rection is made from Eq. (8), a region of very low wind speeds may lead

to an unrealistic correction distance. Further, because the distance

of correction is relatively large for a given value of δM, in such cases,

FIG. 1. Analysis of Montgomery stream function (10^7 erg g^{-1}) at $\theta = 300$K for 22 November 1962, 1200 GMT. Pressures at $\theta = 300$K are plotted. Enclosed region is area of trajectory computations.
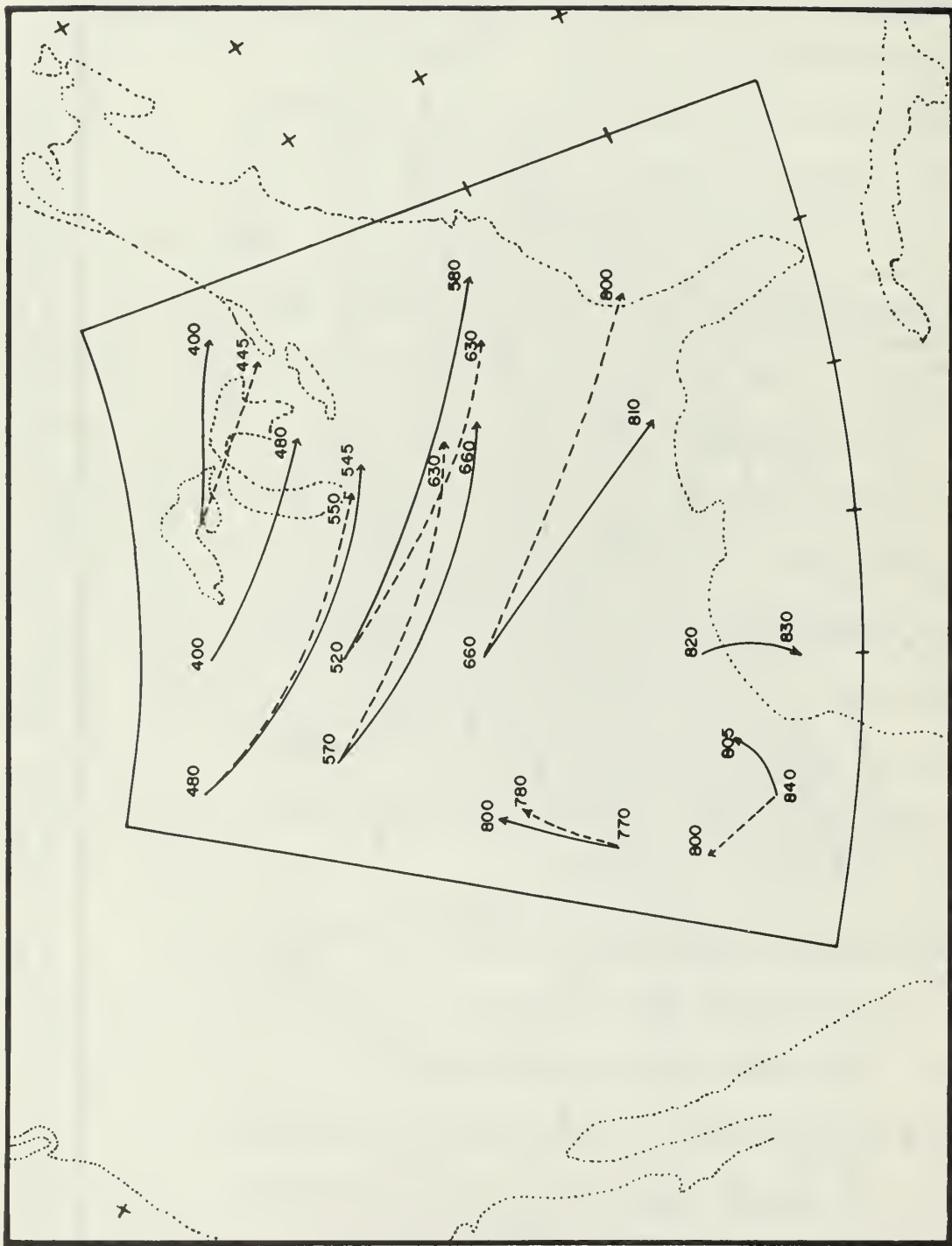
15

Fig. 2. Selected isentropic trajectories at $\theta = 300$ K from 22 November 1200 GMT to 23 November 0000 GMT, 1962. Dashed lines represent the kinematic trajectories computed directly from the wind field. Solid lines are the energy iterated trajectories. If no dashed line is present, the kinematic trajectory also satisfies the integral condition of Eq. 5. Pressures are given at initial and final trajectory points.

the correction is particularly sensitive to analysis errors in the M fields.
Thus in this case, the "corrected" trajectory becomes less accurate than
the kinematic trajectory. In this program, and also in graphical calcu-
lations, it has been found to be advantageous to simply use the kinematic
trajectory in cases where the wind speed is less than 10 m sec^{-1}.

Another source of error in the iterative calculations arises when
there exists a very rapid change of wind direction perpendicular to the
estimated trajectory path. In such cases the energy iterated trajectory
direction may differ somewhat from the actual wind direction at the final
point. This type of error also usually occurs when the wind speed it-
self is quite low. As above, the kinematic trajectory is then held to be
the more accurate one.

A final difficulty in the iterative scheme arises when the wind shear
is strongly anticyclonic in the region of the trajectory. In this case the
changes of Montgomery stream function and of kinetic energy are nega-
tively correlated in the iterative correction of an approximate trajectory
using Eq. (5). For example, a correction to increase the value of M_f
will simultaneously cause a marked reduction in the final kinetic energy.
A result the computation may be left as far from convergence as in the previous
approximation. Occasionally the iteration may even diverge from the true
solution. In such cases the kinematic trajectory is again used as the
better approximation to the true trajectory.

In regions where the above difficulties are not present, the iterative

procedure gives very acceptable results for adiabatic trajectory calculations. The inclusion of diabatic effects produces considerable additional complication and will be discussed in the subsequent section.

4. Incorporation of diabatic effects into trajectory determinations

Although the air flow in the free atmosphere tends to be roughly adiabatic in character, diabatic effects are always present. At times these diabatic effects may lead to a true trajectory which is appreciably different than that obtained by assuming isentropic conditions.

At first it might seem to be contradictory to consider diabatic effects within the framework of a problem formulated in isentropic coordinates. However, even for diabatic trajectories, the θ coordinate system retains its advantage over Z or p coordinates for several reasons. First, the adiabatic component of vertical motion is invariably larger than the diabatic part. This implies that the relative distance a parcel will "depart" from its original isentropic surface is appreciably smaller than the departure from a Z or p surface. Second, the diabatic effect of release of latent heat of a parcel is strongly dependent upon the cooling of an air parcel due to adiabatic ascent. Thus, an accurate determination of the three dimensional motion of a parcel is logically obtained by utilizing an initial knowledge of the adiabatic part of the vertical motion.

This fact will now be used to develop a method for evaluating the diabatic components of the motion as an extension of the isentropic

18

method outlined in previous sections. From the definition of a mean value,

$$\bar{\omega}\,\Delta t = \int_{t_1}^{t_2} \frac{dp}{dt}dt \approx \int_{t_1}^{t_2} \frac{dp}{dt}_{ad}\,dt + \int_{t_1}^{t_2} \frac{dp}{dt}_{lr}\,dt + \int_{t_1}^{t_2} \frac{dp}{dt}_{lh}\,dt \qquad (12)$$

where $\omega = dp/dt$, dp/dt_{ad} is the adiabatic part of ω, dp/dt_{lr} is the contribution to ω from long wave cooling, and dp/dt_{lh} is the ω due to release of latent heat of condensation.

However, the second and third terms on the right hand side of Eq. (12) represent a pressure change due only to a change of potential temperature of the parcel. Thus one may write,

$$\bar{\omega}\,\Delta t = \Delta p_{ad} + \overline{\frac{\partial p}{\partial \theta}}\,\Delta \theta_{lr} + \overline{\frac{\partial p}{\partial \theta}}\,\Delta \theta_{lh} \qquad (13)$$

where $\overline{\partial p/\partial \theta}$ is the measure of the mean static stability along the trajectory and $\Delta \theta$ is the change of potential temperature. Thus, in this model the total vertical displacement of an air parcel is due to a combination of three effects, only the first of which is available from the method described previously. The term in Eq. (13) involving $\Delta \theta_{lr}$ can be extremely complex to evaluate, since it, in general, includes long wave radiative effects of water vapor, ozone and carbon dioxide. However, the contribution of ozone is very small in the troposphere. Also, according to Manabe and Möller (1961) the contribution of carbon dioxide is considerably smaller than that of water vapor.

Making use of the above fact, Danard (1968) has developed a technique for computing the long wave cooling due to an arbitrary cloud

19

and moisture distribution. Danard's model has been adapted for application to this problem. Fig. 3 shows diabatic cooling rates (deg. C/12 hr) computed from Danard's model and interpolated to the $\theta = 300K$ surface for 22 November 1200 GMT. This figure shows that the spatial variation of diabatic cooling on a θ surface is surprisingly large. Cooling rates in excess of 2 deg/12 hr are observed in the northeast corner. These high values are due to radiation from the top of the cloud cover on the east side of the trough observed in Fig. 1. Note also the low cooling rates in the central part of Fig. 3. This area is within and behind the base of the trough and has been shown to be a large mass of descending dry stratospheric air in a previous paper (Reiter and Mahlman, 1965c). Another reason for the pronounced variability of the cooling rates is due to the large slope of the $\theta = 300K$ surface. In this case the pressure varies from 920 to 400 mb, thus leading to large variations of height and temperature over the map. It may be seen, however, that this method contains the possibility of gaining a more adequate determination of the diabatic cooling of a parcel due to long wave radiation. The most straightforward way to include this in a trajectory calculation would be to simply use the average of the cooling rates computed at the initial and final points of the adiabatic trajectory.

The last term in Eq. (13) represents the contribution to the total pressure change of a parcel due to release of latent heat of condensation. This, of course, is a heating effect and tends to balance the diabatic cooling due to long wave radiation. The heating of an air parcel due
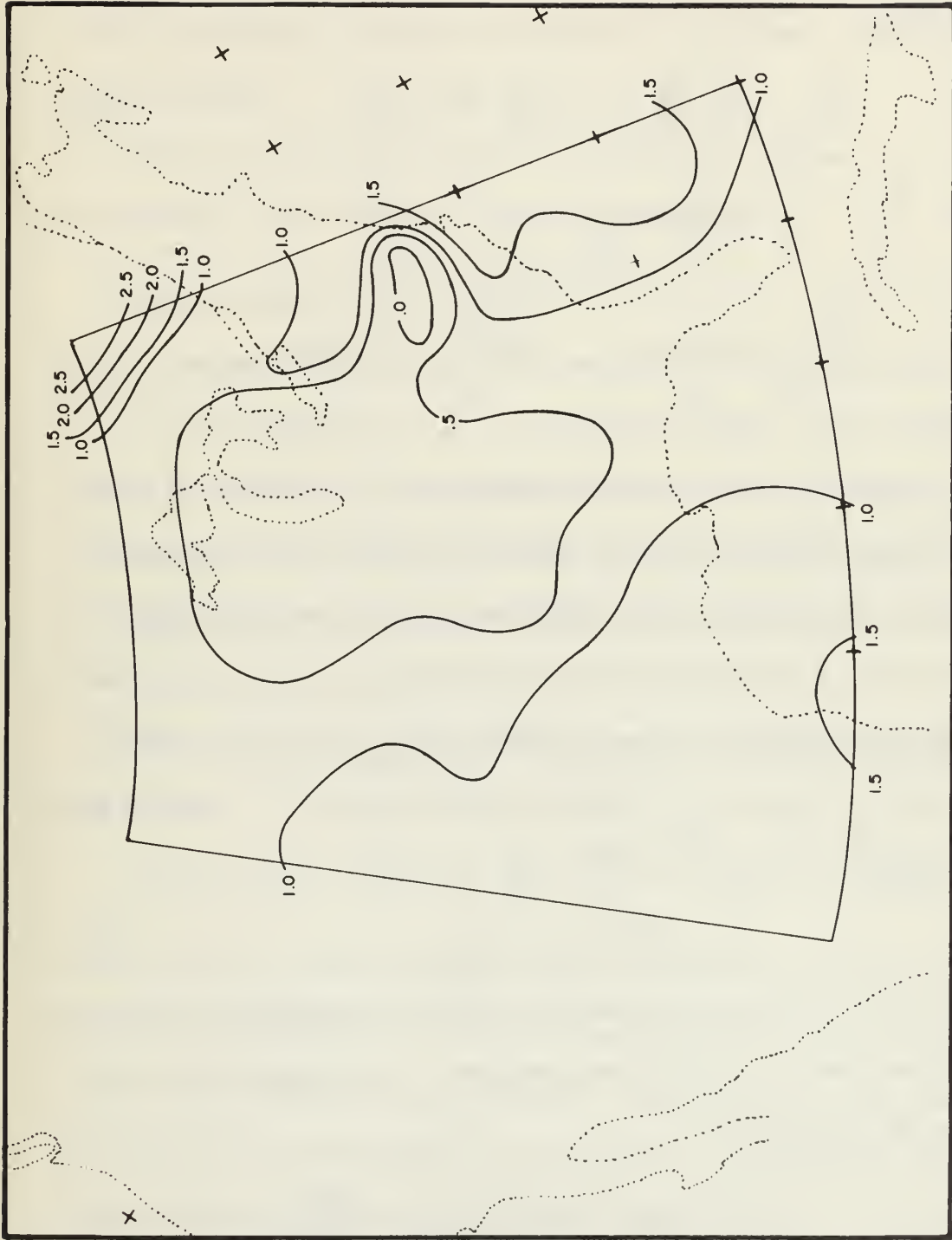
FIG. 3. Computed diabatic cooling rates for 22 November 1962, 1200 GMT at $\theta = 300K$. Units are expressed in deg C/12 hr. Strong cooling rates at eastern edge are due to cloud top radiation. Low cooling rates in central region are associated with the dry descending air in this region.

to condensation of water vapor may be written with sufficient approximation as

$$\frac{dH}{dt}_{lh} = \frac{c_p T}{\theta} \frac{d\theta}{dt}_{lh} \approx L \omega \frac{\partial q_s}{\partial p} \, \delta(x,y,\theta,t) \tag{14}$$

where $\frac{dH}{dt}_{lh}$ is the heating due to release of latent heat, L the latent heat

of vaporization, $\partial q_s/\partial p$ the rate of change of saturation specific

humidity with respect to pressure and $\delta(x,y,\theta,t)$ is either one or zero

depending upon whether the point x, y, θ, t is saturated or not.

To obtain the actual value of heating of a parcel over a 12 hour

time interval due to latent heat release, Eq. (14) must be integrated

over $\Delta t'$, the interval of time which the parcel is saturated. This

value of $\Delta t'$ is determined by first determining the initial value of q

for the parcel and then finding the pressure (p_{sat}) at the θ surface

for which the value of q_s equals the initial value of q. From this one

may define

$$\Delta p' = p_i - p_{sat} \tag{15}$$

where $\Delta p'$ is the pressure change a parcel must undergo to experience

saturation, and p_i is the initial pressure. Eq. (15) may then be used

to form the expression

$$\Delta t' = t_f - t' = 12 \left(1 - \frac{\Delta p'}{(\Delta p_{ad} + \frac{\partial p}{\partial \theta} \Delta \theta_{lr})} \right), \tag{16}$$

where, if $\Delta t'$ is less than zero, it is set to be zero for the computation.

Here, $(\Delta p_{ad} + \overline{\frac{\partial p}{\partial \theta}} \Delta \theta_{lr})$ represents the total 12 hour pressure change experienced by the parcel due to the effects of adiabatic motion and long wave radiation.

One may now integrate Eq. (14) over the time interval $\Delta t'$ to obtain

$$\Delta \theta_{lh} = - \int_{t'}^{t_f} \frac{\theta L \omega}{c_p T} \frac{\partial q_s}{\partial p} dt, \quad \text{or} \tag{16a}$$

$$\Delta \theta_{lh} = \frac{-1000^{\varkappa} L}{c_p} \frac{\overline{\omega \frac{\partial q_s}{\partial p}}}{p^{\varkappa}} \Delta t' \approx \frac{1000^{\varkappa} L}{c_p} \frac{\overline{\omega}}{p^{\varkappa}} \frac{\overline{\partial q_s}}{\partial p} \Delta t', \tag{16b}$$

where $\varkappa = 0.2857$. The approximation in Eq. (16b) is justified <u>because</u> all terms involving deviations from the mean in the expansion of $\omega \, \partial q_s / \partial p / p^{\varkappa}$ are more than one order of magnitude smaller than the term retained.

If the expression for $\Delta \theta_{lh}$ in Eq. (16b) is substituted into Eq. (13), one obtains

$$\overline{\omega}_1 \Delta t = \Delta p_{ad} + \overline{\frac{\partial p}{\partial \theta}} \Delta \theta_{lh} - \overline{\frac{\partial p}{\partial \theta}} \frac{1000^{\varkappa} L}{c_p} \frac{(\overline{\omega}_{ad} + \overline{\omega}_{lh})}{p^{\varkappa}} \frac{\overline{\partial q_s}}{\partial p} \Delta t' \tag{17}$$

Note that the $\overline{\omega}$ values obtained from the adiabatic trajectory and the long wave cooling effect are used as the initial approximation to the true $\overline{\omega}$ field required in the third term. The subscript on $\overline{\omega}_1$ denotes that this is the first approximation to the total pressure change by the parcel. Eq. (17) can now be solved iteratively for the final mean ω by writing

$$\overline{\omega}_{n+1} \Delta t = \Delta p_{ad} \div \overline{\frac{\partial p}{\partial \theta}} \Delta \theta_{lr} - \overline{\frac{\partial p}{\partial \theta}} \frac{1000^{\varkappa} L}{c_p} \frac{\overline{\omega}_n}{p^{\varkappa}} \frac{\overline{\partial q_s}}{\partial p} \Delta t', \tag{18}$$

23

where the n subscript indicates the number of iterations. This iteration can be continued until $|\bar{\omega}_{n+1} - \bar{\omega}_n| < \epsilon$, where ϵ is some acceptable error. The mean vertical motion over the 12 hour period has now been obtained. Now that the total vertical displacement has been obtained, the total diabatic heating of a parcel is given by the expression

$$\Delta\theta = \Delta\theta_{lr} - \frac{1000^{\mathcal{X}_L}}{c_p} \frac{\bar{\omega}_{n+1}}{\bar{p^{\mathcal{X}}}} \overline{\frac{\partial q_s}{\partial p}} \Delta t', \tag{19}$$

where $\Delta\theta$ determined along the trajectory. An interpolation in θ is utilized to find wind speeds at each new potential temperature along the path. Utilizing these new values, a correction is then made for distance according to Eq. (10).

To begin preparation for the lateral correction of the diabatic trajectory, $\Delta\theta$ from Eq. (19) is substituted into term (4) of Eq. (5) written as

$$\int_{\theta_i}^{\theta_f} \frac{\partial}{\partial\theta}\left(\frac{V^2}{2}\right) d\theta = \overline{\frac{\partial}{\partial\theta}\left(\frac{V^2}{2}\right)} \Delta\theta. \tag{20}$$

The vertical derivative of the kinetic energy is evaluated along the trajectory by a centered finite difference of the kinetic energies of the levels above and below the parcel at a given point along the trajectory.

The computed value from Eq. (20) is then substituted into Eq. (5) to obtain a new computed value of M_f for the trajectory. A lateral correction is then made for the trajectory in the same manner as done previously for the adiabatic case. This correction is normally small because the numerical value obtained from Eq. (2) is nearly always less than $.2 \times 10^7$ erg g^{-1} -- considerably smaller than the usual magnitude of terms (1), (2), or (3) in

24

Eq. (5).

If this correction is small enough that the computed and observed values of M_f agree within the predetermined limits, the trajectory is complete and simultaneously satisfies the energy equation and the diabatic effects.

Provided that a correction is necessary in order to satisfy Eq. (5), the next step is to provide an additional correction for the change of distance along the trajectory due to effects of horizontal wind shear. This corrected trajectory is then checked by a recomputation of Eq. (5). If the computed and observed values of M_f (projected from the diabatic trajectory onto the original θ surface) do not agree within the predetermined limits, this process is repeated until the convergence criterion is satisfied.

However, even though Eqs. (5) and (6) are now satisfied for this new trajectory, the possibility remains that the computed vertical displacement is again in error, since a path correction has been made. A new check is accomplished by recycling through the process outlined from Eq. (14) through Eq. (18). If $\overline{\omega}_{n+1}$ is sufficiently close to the previous value of $\overline{\omega}_{n+1}$ obtained from the first cycle, the trajectory is complete. If these two computed values differ appreciably, the cyclic procedure beginning with Eq. (19) is repeated until one of the exit criteria is satisfied.

At the present time little quantitative information is available as to the number of cycles required for the computed trajectory to satisfy the

25

convergence criteria. In a set of graphical computations of diabatic effects on trajectories by the author in a previous publication (Reiter et. al., 1965), only one to three iterations were normally required. In that computation, conservation of equivalent potential temperature was imposed as an additional criterion to be satisfied along the trajectory.

Although there are no fundamental difficulties in programming the inclusion of diabatic effects for machine computation, in actual practice this will prove to be very difficult and time consuming. Further, it should be noted that this method will be incapable of determining trajectories in areas dominated by sub-synoptic scale motions.

5. Summary

A working computer method has been outlined for objective computation of isentropic trajectories in the free atmosphere using a modification of the scheme originally derived by Danielsen (1961). This method has been found to give highly acceptable results in most cases. The method was found to give poor results in either areas of very low wind speeds or regions characterized by strong anticyclonic wind shears.

A general technique for expanding this method for inclusion of diabatic flows has been presented in some detail. This should enable investigation of more general three-dimensional flow problems than have been capable of solution up to the present time. The required expansions of the isentropic trajectory program to include diabatic effects are currently in progress.

6. Literature Cited

Danielsen, E. F., 1959: The laminar structure of the atmosphere and its relation to the concept of a tropopause. Archiv für Meteorologie, Geophysik und Bioklimatologie, A11, 293-332.

_____, 1961: Trajectories: isobaric, isentropic, and actual. Journal of Meteorology, 18, 479-486.

_____, 1964: Radioactivity transport from stratosphere to troposphere. Mineral Industries, 33, 1-7.

_____, K. H. Bergman, and C. A. Paulson, 1962: Radioisotopes, potential temperature and potential vorticity -- a study of stratospheric-tropospheric exchange processes. Department of Meteorology and Climatology, University of Washington, 54 pp.

Danard, M. B., 1968: On the inclusion of long wave radiation in a tropospheric numerical prediction model. Scientific Report No. 1 to Air Force Cambridge Research Laboratories, (MIPR-ES-7-967), Naval Postgraduate School, 17 pp.

Djuric, D., 1961: On the accuracy of air trajectory computations. Journal of Meteorology, 18, 597-605.

Houghton, D. D., 1962: A calculation of the large scale three-dimensional distribution of diabatic heating in the atmosphere. Archiv für Meteorologie, Geophysik und Bioklimatologie, A12, 407-425.

Krishnamurti, T. N., 1966a: A study of wave cyclone development. Diagnostic Studies of Weather Systems of Low and High Latitudes (Rossby

Number < 1), Final Report for Air Force Cambridge Research Laboratories, (AF 19(628)-4777), 52 pp.

_____, 1966b: A diagnostic balance model for studies of weather systems of low and high latitudes. Diagnostic Studies of Weather Systems of Low and High Latitudes (Rossby Number < 1), Final Report for Air Force Cambridge Research Laboratories, (AF 19(628)-4777), 41 pp.

Kung, E. C., 1967: Diurnal and long-term variations of the kinetic energy generation and dissipation for a five year period. Monthly Weather Review, 95, 593-606.

Mahlman, J. D., 1965: Relation of stratospheric-tropspheric mass exchange mechanisms to surface radioactive peaks. Archiv für Meteorologie, Geophysik und Bioklimatologie, A15, 1-25.

Manabe, S., and F. Möller, 1961: On the radiative equilibrium and the heat balance of the atmosphere. Monthly Weather Review, 89, 503-532.

Nagle, R. E. and J. R. Clark, 1966: Interpretative uses of the diagnostic cycle routine. Final Report for Environmental Science Services Administration (CWB-11254), Meteorology International, 43 pp.

Paegle, J., 1966: Numerical calculation of three dimensional trajectories utilizing the balanced horizontal and vertical motions. Diagnostic Studies of Weather Systems of Low and High Latitudes (Rossby Number < 1), Final Report for Air Force Cambridge Research Laboratories, (AF 19(628)-4777), 21 pp.

Palmén, E., and C. W. Newton, 1951: On the three-dimensional motions in an outbreak of polar air. Journal of Meteorology, 8, 25-39.

Panofsky, H. A., 1946: Methods of computing vertical motion in the atmosphere. Journal of Meteorology, 3, 45-49.

Petterssen, S., 1956: Weather Analysis and Forecasting, Vol. 1. McGraw-Hill, New York, 428 pp.

Reiter, E. R., 1963: A case study of radioactive fallout. Journal of Applied Meteorology, 2, 691-705.

_____, and E. F. Danielsen, 1960: Bemerkungen zu E. Kleinschmidt: "Nicht-adiabatische Abkühlung im Bereich des jet stream". Beiträge zur Physik der Atmosphäre, 32, 265-273.

_____, D. W. Beran, J. D. Mahlman, and G. Wooldridge, 1965: Effect of large mountain ranges on atmospheric flow patterns as seen from TIROS satellites. Atmospheric Science Technical Paper No. 69, Colorado State University, 86 pp.

_____, and J. D. Mahlman, 1965a; Heavy iodine - 131 fallout over the midwestern United States, May 1962. Atmospheric Science Technical Paper No. 70, Colorado State University, 1-53.

_____, and J. D. Mahlman, 1965b: A case study of mass transport from stratosphere to troposphere, not associated with surface fallout. Atmospheric Science Technical Paper No. 70, Colorado State University, 54-83.

_____, and J. D. Mahlman, 1965c: Heavy radioactive fallout over the southern United States, November 1962. Journal of Geophysical Research, 70, 4501-4520.

Saucier, W. J., 1955: _Principles of Meteorological Analysis_. The

    University of Chicago Press, Chicago, 438 pp.

Staley, D. O., 1960: Evaluation of potential vorticity changes near the

    tropopause and related vertical motion, vertical advection of

    vorticity, and the transfer of radioactivity from the stratosphere to

    the troposphere. _Journal of Meteorology_, 17, 591-620.

_____, 1962: On the mechanism of mass and radioactivity transport

    from stratosphere to troposphere. _Journal of the Atmospheric

    Sciences_, 19, 450-457.

DOCUMENT CONTROL DATA - R & D

Security classification of title, body of abstract and indexing annotation must be entered when the overall report is classified)

1. ORIGINATING ACTIVITY *(Corporate author)*	2a. REPORT SECURITY CLASSIFICATION
Naval Postgraduate School Department of Meteorology and Oceanography Monterey, California 93940	Unclassified
	2b. GROUP

3. REPORT TITLE

NUMERICAL METHODS OF COMPUTING THREE-DIMENSIONAL TRAJECTORIES FOR ADIABATIC AND DIABATIC FLOWS.

4. DESCRIPTIVE NOTES *(Type of report and, inclusive dates)*

Scientific   Interim.

5. AUTHOR(S) *(First name, middle initial, last name)*

J. D. Mahlman

6. REPORT DATE	7a. TOTAL NO. OF PAGES	7b. NO. OF REFS
August 1968	35	25

8a. CONTRACT OR GRANT NO	9a. ORIGINATOR'S REPORT NUMBER(S)
MIPR ES-7-967	NPS-51MZ8061A
b. PROJECT NO. Task, Work Unit Nos. 6698-02-01	Scientific Report No. 3
c. DoD Element 62405394	9b. OTHER REPORT NO(S) *(Any other numbers that may be assigned this report)*
d. DoD Subelement 681000	AFCRL-68-0357

10. DISTRIBUTION STATEMENT

1-Distribution of this document is unlimited. It may be released to the Clearinghouse Department of Commerce, for sale to the general public.

11. SUPPLEMENTARY NOTES	12. SPONSORING MILITARY ACTIVITY
TECH, OTHER	Air Force Cambridge Research Laboratories(CRE L. G. Hanscom Field, Bedford, Massachusetts 01730

13. ABSTRACT

A computer method for objective computation of adiabatic three-dimensional trajectories in the free atmosphere is presented. This technique utilizes a digital adaption of the graphical iterative method introduced by Danielsen (1961).

The program is applied to a test case and is found to give generally satisfactory results. Some difficulties are encountered in cases of very low wind speeds and also in regions of strong anticyclonic wind shears.

A method for inclusion of diabatic effects is outlined in detail. This approach may allow investigation of more complicated flow problems than have been previously possible.

DD FORM 1473 (PAGE 1)
1 NOV 65

S/N 0101-807-6811

Unclassified
Security Classification

A-31408

KEY WORDS	LINK A		LINK B		LINK C	
	ROLE	WT	ROLE	WT	ROLE	WT
Three-dimensional trajectories						
Adiabatic and diabatic flows						
Energy equation						

U120091